Colloids and Surfaces B: Biointerfaces 146 (2016) 785–793

Contents lists available at ScienceDirect

Colloids and Surfaces B: Biointerfaces

journal homepage: www.elsevier.com/locate/colsurfb

Substrate effect modulates adhesion and proliferation of fibroblast on graphene layer

Feng Lin[a,1], Feng Du[a,1], Jianyong Huang[a,b], Alicia Chau[c], Yongsheng Zhou[d,e], Huiling Duan[a,f], Jianxiang Wang[a,f,*], Chunyang Xiong[a,c,*]

[a] State Key Laboratory for Turbulence and Complex System, and Department of Mechanics and Engineering Science, College of Engineering, Peking University, Beijing 100871, China
[b] Department of Biomedical Engineering, Duke University, Durham, NC, 27708, USA
[c] Academy for Advanced Interdisciplinary Studies, Peking University, Beijing 100871, China
[d] Department of Prosthodontics, Peking University School and Hospital of Stomatology, Beijing 100081, China
[e] National Engineering Laboratory for Digital and Material Technology of Stomatology, Beijing 100081, China
[f] CAPT-HEDPS, and IFSA Collaborative Innovation Center of MoE, Peking University, Beijing 100871, China

ARTICLE INFO

Article history:
Received 2 May 2016
Received in revised form 4 July 2016
Accepted 4 July 2016
Available online 5 July 2016

Keywords:
Graphene
Cytocompatibility
Cell function and behavior
Substrate stiffness
Surface wetting property

ABSTRACT

Graphene is an emerging candidate for biomedical applications, including biosensor, drug delivery and scaffold biomaterials. Cellular functions and behaviors on different graphene-coated substrates, however, still remain elusive to a great extent. This paper explored the functional responses of cells such as adhesion and proliferation, to different kinds of substrates including coverslips, silicone, polydimethylsiloxane (PDMS) with different curing ratios, PDMS treated with oxygen plasma, and their counterparts coated with single layer graphene (SLG). Specifically, adherent cell number, spreading area and cytoskeleton configuration were exploited to characterize cell-substrate adhesion ability, while MTT assay was employed to test the proliferation capability of fibroblasts. Experimental outcome demonstrated graphene coating had excellent cytocompatibility, which could lead to an increase in early adhesion, spreading, proliferation, and remodeling of cytoskeletons of fibroblast cells. Notably, it was found that the underlying substrate effect, e.g., stiffness of substrate materials, could essentially regulate the adhesion and proliferation of cells cultured on graphene. The stiffer the substrates were, the stronger the abilities of adhesion and proliferation of fibroblasts were. This study not only deepens our understanding of substrate-modulated interfacial interactions between live cells and graphene, but also provides a valuable guidance for the design and application of graphene-based biomaterials in biomedical engineering.

1. Introduction

As a new two-dimensional material, graphene has recently been thought of as a perfect candidate for biomedical application due to its unique properties [1–5]. For example, it has been used as a coating material in tissue engineering for its exceptional antibacterial activity and high cytocompatibility [6–8]. Previously, it was found that homogenous graphene substrates played a key role in regulating cell functions and behaviors. For instance, single layer graphene (SLG), which was produced by chemical vapor deposition (CVD), increased the adhesion of osteoblasts and hMSCs (human mesenchymal stem cells) [9]. It has been recognized that micropatterned CVD SLG substrates can not only significantly enhance the adhesion and growth of neuron [10], but also accelerate the osteogenic differentiation of hMSCs [11–13].

It is well known that graphene has to be supported on a substrate for cell culture and tissue engineering application. In fact, the published results of graphene's exceptional cytocompatibility were mostly supported by an underlying SiO_2 or glass substrate, which was also suitable for cell culture. Simultaneously, recent progresses have revealed that the underlying substrate can exert a remarkable impact on the surface properties of graphene. It has been reported that, for instance, the wetting property of graphene was tuned by its underlying substrate [14,15]. The adsorption ability [16,17], morphology [18] and apparent mechanical properties [19] of graphene

* Corresponding authors at: State Key Laboratory for Turbulence and Complex System, and Department of Mechanics and Engineering Science, College of Engineering, Peking University, Beijing 100871, China.
E-mail addresses: jxwang@pku.edu.cn (J. Wang), cyxiong@pku.edu.cn (C. Xiong).
[1] These authors contributed equally.

http://dx.doi.org/10.1016/j.colsurfb.2016.07.008
0927-7765/

were also closely related to the underlying substrates. So it is reasonable to speculate that graphene-induced cytocompatibility may be also regulated by the properties of its underlying substrates.

In the current work, different substrates, including widely used glass, commercially available silicone sheets, and polydimethylsiloxane (PDMS), with or without SLG-coating were prepared to investigate the effect of the underlying substrate on graphene-induced adhesion and proliferation of NIH-3T3 fibroblasts. Two curing ratios of PDMS substrates with different stiffness were used (stiffer mixture of 10:1 and softer mixture of 50:1, referred as P10 and P50, respectively). Further, in order to investigate the influence of substrate wetting property on graphene-induced cell adhesion and proliferation, P10 was modified by oxygen plasma (hereafter referred as p-P10). Then, the behaviors were investigated, including early adhesion of cell, morphology, cytoskeleton structure and proliferation of fibroblasts. The experimental results demonstrated that graphene improved the substrate cytocompatibility even if the bare substrate was not originally suitable for cell growth. Notably, the fibroblasts adhesion and proliferation were not completely equivalent in all SLG-coated substrates; especially the graphene-induced fibroblasts adhesion and proliferation on softer substrates were lower than that on stiffer substrates significantly. These findings imply that the underlying substrates can exert a conspicuous effect on graphene-induced adhesion and proliferation of fibroblasts. It deepens our understanding of interfacing live cells with graphene, which provides a valuable guidance for the design and application of graphene-based materials in tissue engineering.

2. Materials and methods

2.1. Materials and reagents

SLG on copper foil grown by CVD was purchased from ACS Materials (Massachusetts, USA). Glass coverslips (thickness range: 0.13–0.17 mm) were purchased from VWR (West Chester, USA). PDMS (Sylgard 184) was bought from Dow Corning (Michigan, USA). Commercial silicone sheets (~250 μm in thickness; SM08111321) were purchased from SMI (Michigan, USA). Polymethylmethacrylate powder (PMMA, molecular weight: 996000) was obtained from Sigma-Aldrich (182265, St. Louis, Mo, USA). Ammoniumpersulfate (APS), hydrogen peroxide, sulfuric acid, ethanol and acetone were bought from Beijing Chemical Reagent Company (Beijing, China). All these chemicals were used as received.

2.2. Preparation of bare substrates

Glass substrates were cleaned before used by immersing into piranha solution (hydrogen peroxide (30%)/sulfuric acid 1:3) for 10 min at 120 °C, washed with deionization (DI) water and ethanol, and then dried by blowing nitrogen gas.

PDMS contains two chemical parts, i.e., a PDMS polymer base (A) and a curing agent (B). Different curing ratios of 10:1 and 50:1 were thoroughly mixed and degassed in experiments (referred as P10 and P50, respectively). The PDMS mixture was subsequently poured onto a cover glass and heated at 70 °C for 6 h in an oven to accelerate the polymerization and cross-linking.

Oxygen plasma (FEMTO plasma cleaner, 40 kHz frequency) was used to hydrophilic modification of PDMS substrate with the curing ration of 10:1 (referred as p-P10). The system pressure and oxygen flow rate were kept constant at 100 micro-bars and 20 sccm (standard cubic centimeters per minute), respectively. The plasma power was set at 60 w and lasted for 30 s.

2.3. Graphene transfer

In order to ensure the integrity of graphene during transferring, and simultaneously consider the different properties of the underlying substrates, two different methods were chosen to transfer graphene. The first method was based on directly adhering graphene from copper foil for the flexible and hydrophobic substrates, such as silicon, P10 and P50 used in this study [20,21]. Both sides of as-grown CVD graphene on 25 μm thick copper foils were covered by graphene. In order to remove one side of graphene, a piece of graphene covered copper foil was pressed on a flat substrate gently to make it as possible as flat, PDMS film was then cut into strips and used to seal the copper foil boundary on a flat glass plate. The graphene was destroyed with the treatment of Oxygen plasma of 100 W for 3 min. Then we used PDMS or silicone samples to adhere the other side of the copper foil. To make it adhere firmly, it was necessary to make sure the copper foil was flat. Then relatively dilute APS solution of 0.5 M was adopted to etch the copper. After copper foil was etched completely, the sample was washed with flowing DI water and drying by a weak flow from a nitrogen gun.

The other transfer method was based on widely used PMMA transfer technique for common solid and hydrophilic substrates, for instance glass and p-P10 used in the present experiments [22,23]. In short, a thin protective layer of PMMA was spin coated at 500 rpm for 20 s and 2000 rpm for 30 s on the copper foil, and then heated on a hot plate at 170 °C for 3 mins. The other side of graphene was removed by oxygen plasma under the same conditions as that utilized in the first method. After copper was etched in APS solution and carefully washed, the floating PMMA-coated graphene film was scooped with glass and p-P10 substrate. The samples were left overnight to dry in ambient condition. The top PMMA coating was stripped off in hot acetone of 50 °C for 30 min and followed by dipping in ethanol to rinse off any residue. SLG-coated substrates were referred as silicone-g, P10-g, P50-g, and p-P10-g, respectively.

2.4. Characterization of various substrates

2.4.1. Raman spectra detects graphene

Raman spectra were carried out using LabRAM ARAMIS System (HR800, HORIBA, Paris, France) equipped with a 532 nm laser source. The laser spot has a diameter of 1 μm. To avoid laser-induced heating and damage to the graphene, the laser power was kept below 2 mW during scanning.

2.4.2. Static contact angle measurements

Static contact angle measurements were performed at room temperature (22–25 °C) at a relative humidity of 27–43% using an automatic contact angle meter (OCA 20, DataPhysics, Stuttgart, Germany). A volume of 2 μL DI water drop was used during the static contact angle measurement. Each group contains five parallel samples and 3 test points were randomly chosen for each sample.

2.4.3. Atomic force microscopy and elastic modulus measurement

The surface morphology of transferred graphene on these various substrates was investigated by atomic force microscope (MFP-3D, Asylum Research, USA) utilizing the tapping mode with a silicon cantilever with a spring constant of ~1.2 N/m and resonance frequency of ~75 kHz. The root mean square roughness (rms) of the images was also evaluated using the integrated software. Five positions were chosen with an area of 5 μm × 5 μm for each position. In the experiment, force-distance curves were also collected to obtain the apparent stiffness of these substrates. For the sphere indentation as adopted here, the Young's modulus was finally quantified via the classical Hertz model [24,25].

2.5. Cell culture

NIH-3T3 (Mouse embryonic fibroblast cell line) cells were cultured in 37 °C, 5% CO_2 incubator with Dulbecco's modification of Eagle's medium (DMEM) supplied with 10% fetal bovine serum (FBS), penicillin (100 U/mL), streptomycin (100 μg/mL). Cells were subcultured at least twice a week when cells grew to 80% confluence.

2.6. Assessment of cell adhesion

The number of adhered cells on these substrates was counted by means of nuclei quantification. Fibroblasts were seeded on bare and SLG-coated different substrates in a 6-well plated with an initial cell density of $\sim 2 \times 10^4$/well. After incubation for 3 h, the seeded cells were gently washed with PBS for three times. The cells were subsequently fixed with 4% paraformaldehyde at room temperature, washed with PBS, and eventually stained with DAPI. Afterwards, the stained cells were counted in five random fields with the aid of an invert fluorescence microscopy (X71, Olympus, Japan). Each group was repeated five times for the purpose of statistical analysis.

2.7. Assessment of cell proliferation

Proliferation of fibroblasts cultured on these different substrates as mentioned above, was measured by MTT (3-[4,5-dimethylthiazol-2-yl]-2, 5-diphenyltetrazolium bromide) assay. In brief, bare and SLG-coated substrates were placed in a 24-well plate with the seeded cell density of 1×10^4/well. Then the cells were cultured for 24 and 48 h under the standard condition of cell culture as stated above. After the addition of MTT solution (5 mg/mL in PBS), the cells were incubated for another 4 h at 37 °C. Finally, the purple formazan was dissolved with dimethyl sulfoxide (DMSO) and measurement of absorbance at 490 nm was carried out.

2.8. Assessment of cell morphology and cytoskeleton structure

Fibroblasts were seeded on both bare and SLG-coated substrates at a density of 2×10^4/dish to assess the influence of the underlying substrate on graphene-induced cell morphology by analyzing the structures of cellular cytoskeleton 24 h after culture. In brief, phase-contrast images of cells cultured on bare and SLG-coated substrates were first taken by an invert fluorescence microscopy (X71, Olympus, Japan). Subsequently, these cells were fixed with 4% paraformaldehyde for ~20 min at room temperature, permeabilized with 0.1% Trition X-100 for 3 min, and treated with blocking solution (1% BSA) for 30 min. To label intracellular F-actin with fluorescent probe, the cells were incubated with TRICT-Phalloidin (Sigma-Aldrich, St. Louis, Mo, USA) for 30 min at room temperature. To label vinculin, the fixed cells were incubated with monoclonal antivinculin antibody (Abcam, Cambridge, UK; 1:200 in 1% BSA) overnight at 4 °C, and then incubated with the secondary antibody, FITC labeled goat anti mouse IgG (ProteinTech, USA; 1:100 in 1% BSA) for 2 h at room temperature. Also, the cells were incubated with DAPI for 15 min at room temperature in order to visualize the cell nucleus. These labeled cells were imaged by laser confocal scanning microscopy (PerkinElmer, USA). As published previously [26], the cell morphology was quantified by analysis of cell areas traced by cell cytoplasmic borders using the NIH ImageJ software, and the number and area of focal adhesions were also collected to further quantify cell cytoskeleton.

2.9. Statistical analysis

Unless otherwise specified, the data results were expressed as means ± standard deviations (SD). Statistical analysis was performed using one-way analysis of variance (ANOVA) followed by Tukey test for multiple groups. A level of p-value less than 0.05 was considered statistically significant.

3. Results and discussion

3.1. Characterization of SLG-coated substrates

Five different substrates including glass, silicone, P10, P50 and p-P10 (as shown in Fig. 1A) were chosen to investigate the substrate effect on graphene-related cytocompatibility. After SLG is transferred onto these substrates, one can easily distinguish the graphene boundary as shown in Fig. 1B. In our experiments, the quality of graphene was quantitatively evaluated by widely used Raman spectroscopy method through analyzing the characteristics of Raman peaks [27]. Fig. 1C showed a representative Raman spectroscopy of SLG covered P10, where the position of the 2D peak was at 2685 cm^{-1} while the half maximum was 32 cm^{-1}. One can realize that the intensity ratio of 2D to G was larger than 2 and that the D peak was very small, suggesting that the graphene was essentially single layer and almost without defects [27]. Likewise, the results of Raman spectroscopy for the other substrates were similar with that of P10 (data not shown), implying that all the graphene transfer on different substrates fulfilled the single-layer requirement technically. X-ray Photoelectron Spectroscopy (XPS) assay was also used to detect the residual molecules. We found that no copper residual could be detected on the surface of SLG-coated substrates (data not shown). To dissect the effect of surface morphology on cell adhesion and proliferation, AFM was also employed to measure the root mean square roughness (RMS) of various bare and SLG covered substrates. As shown in Fig. 1D, the RMS was only ~1.3 nm, indicating that the representative SLG-covered P10 was very flat, even though there existed some local wrinkling. The similar experimental results can be detected for the other SLG-covered substrates with their RMS ranging between 1 and 3.5 nm and the bare substrates with the RMS varying between 0.5 and 4 nm, implying that surface morphology of bare and SLG-coated substrates in present work has little impact on cell adhesion and proliferation according to some previous reports [28].

Likewise, static water contact angle assay was applied to determine the changes in hydrophobicity of these bare substrates after SLG decoration. As seen in Fig. 2A, these bare substrates showed tremendous difference of wetting properties, from ultrahydrophilic to relatively hydrophilic and hydrophobic. It can be found that the underlying substrates can still exert a significant influence on the wetting property to some extent, although the difference in contact angle was potentially diminished after SLG transfer.

Apart from surface morphology and wetting properties, substrate stiffness also regulated cell adhesion and proliferation. Nanoindentation based on AFM was also employed to measure the stiffness of various SLG-covered substrates. As displayed in Fig. 2B, the rigidities of various SLG-covered substrates showed significant differences ranging from 0.5 MPa to 3.5 MPa, owing to that there was remarkable distinction in the Young's moduli between these underlying bare substrates.

3.2. Early adhesion and subsequent proliferation of fibroblast

In our current work, early adhesion behavior of fibroblast was characterized by quantifying the number of adhered cells on these bare and SLG-coated substrates. Fig. 3A showed the typical distributions of adhered cells on the substrates involved, in which the blue dots represented cell nuclei stained by DAPI, whereas Fig. 3B exhibited the corresponding adhesion ratios. It can be found that there

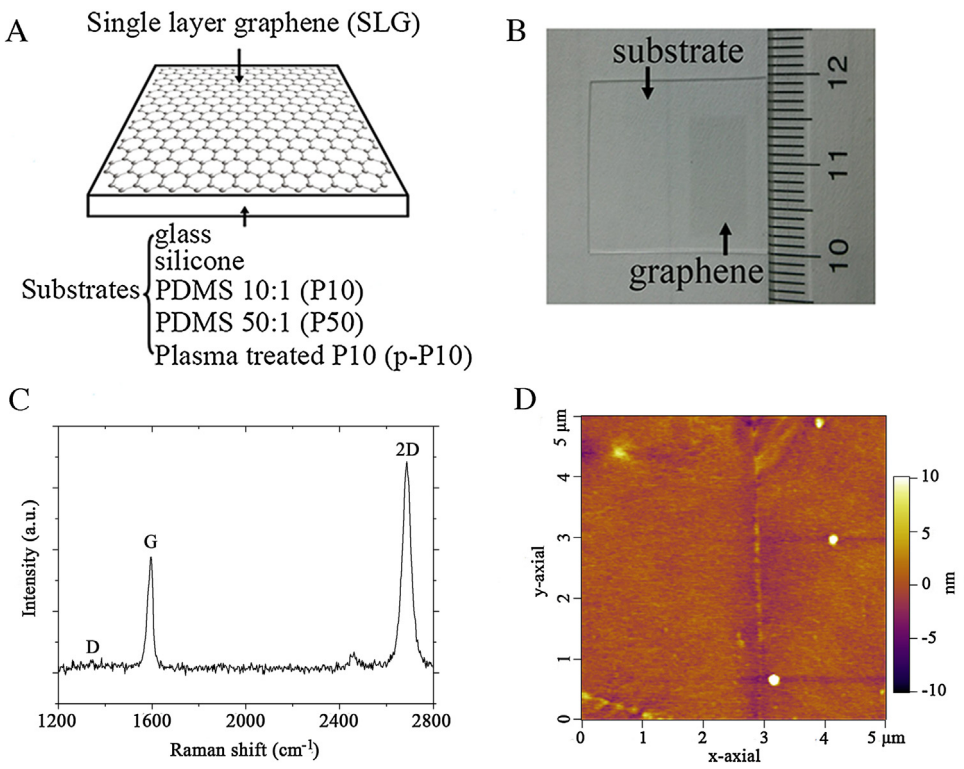

Fig. 1. Schematic diagram and characterization of single layer graphene (SLG) on different substrates. (A) Schematic diagram depicting SLG transferred onto different substrates. (B) Representative optical image of SLG coated substrate. (C) Representative Raman spectra of SLG coated P10. (D) Representative surface topography image of SLG on P10 acquired by AFM in tapping mode with color coded height profile.

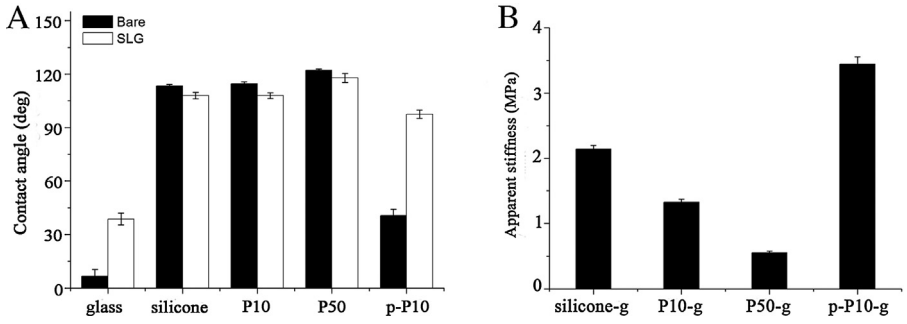

Fig. 2. Characterization of SLG on different substrates. (A) Quantitative sessile drop water contact angle of either or not SLG coated different substrates. (B) Apparent stiffness of SLG-coated different substrates, the columns from left to right showed silicone, P10, P50, and p-P10, respectively. The data were showed as means ± standard deviations (SD) and each group was repeated for five times.

existed significantly difference for the adhesion ability of fibroblast on the bare substrates. In the stiffer and hydrophilic substrates, i.e., bare glass and p-P10, the adhesion was higher than that in softer and hydrophobic substrates, i.e., bare silicone, P10 and P50. Fibroblast adhesion ability was significantly increased after covering with SLG, irrespective of the types of the underlying bare substrates, as displayed in Fig. 3B and C showed the relative proliferation ability of fibroblast incubated on bare and SLG-covered substrates. It can be observed from the experimental results that fibroblast proliferation on stiffer and hydrophilic substrates (glass, silicone and p-P10) was larger than that on softer and hydrophobic substrates (P10 and P50). Similar with the effect of SLG on fibroblast adhesion, fibroblast proliferation on SLG-coated substrates was significantly increased when compared to that on bare substrates.

Apart from the wetting properties, the substrate stiffness had long been deemed as another key factor in influencing various cell behaviors [29–31]. It can be learned that fibroblasts adhesion and proliferation on SLG-covered softer substrate (P50) were significantly lower than those on SLG-coated stiffer substrates (P10 and p-P10, $p < 0.001$). The stiffness value of both bare and SLG-coated glass substrates are several tens of GPa, which is far beyond the stiffness range that can be sensed by cells according to the previous study [32], so the influence of glass stiffness on fibroblasts adhesion and proliferation was not discussed in current work. It has been demonstrated that cells had the ability to feel the depth of the underlying elastic substrates varying from several microns to tens of microns [33,34]. In the present experiments, SLG layer only has a thickness of ~0.34 nm [35], which is at least four orders of magnitude smaller than the thickness cell can feel. In this context, one may imagine that the elastic substrates beneath SLG can have a latent influence on adhesion and proliferation of cells.

3.3. Spreading and cytoskeleton structure

Fig. 4A exhibited some typical phase-contrast images of fibroblasts adhered on these bare and SLG-covered substrates involved,

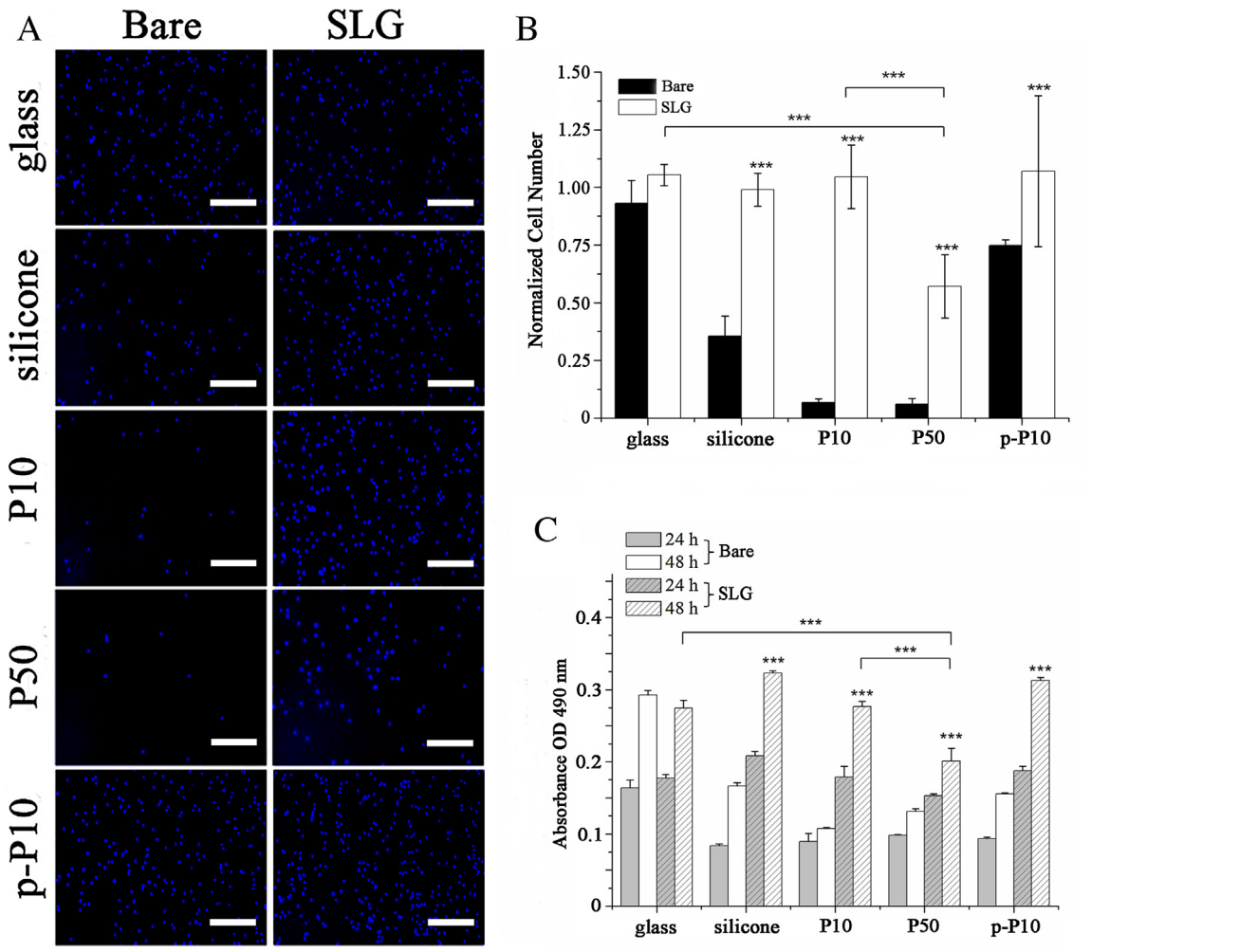

Fig. 3. Early adhesion and proliferation of NIH-3T3 fibroblasts on either or not SLG coated different substrates. (A) Representative images of early adhesion of NIH-3T3 fibroblasts that was characterized by nucleus labeled by DAPI. (B) The relative cell adhesion ratio of the quantitative nucleus number of fibroblasts corresponding to the images shown in (A) to that of culture dish. The results showed that graphene significantly increased the early adhesion of fibroblasts, relating to the stiffness of underlying substrate. (C) NIH-3T3 fibroblast cell proliferation cultured on bare and SLG-coated different substrates for 24 h and 48 h measured by MTT assay. The results showed that graphene significantly increased the cell proliferation, and which was regulated by underlying substrate stiffness, scare bare = 50 μm. (***$p < 0.001$, n = 5).

from which one can readily find the fibroblast spreading was significantly different. Further, Fig. 4B displayed the statistical results about fibroblast spreading area, from which it can be seen that the spreading area was relatively large on stiffer substrates (~2500 μm^2 for bare glass and p-P10 substrates in our experiments), but became less when cultured on softer ones (up to ~1500 μm^2 for bare silicone and P10). The minimum spreading area was observed on the softest substrate (~1000 μm^2 for bare P50).

Additionally, it can be realized that fibroblasts spreading area was enhanced after coating with SLG, whatever the underlying substrate was. Especially, it can be seen that SLG coating could lead to a significant increase in fibroblasts spreading area for P10 and P50 substrates ($p < 0.001$ and 0.01 compared to bare P10 and P50, respectively). However, the spreading extent on SLG-covered P50 was still significantly lower than that on other SLG-covered stiffer substrates (~1800 μm^2 vs. ~3000 μm^2, $p < 0.001$), suggesting that SLG cannot cover all properties of its underlying substrate when supporting fibroblasts spreading.

Considering the fact that cytoskeleton structure plays a key role in regulating various cell behaviors, we simultaneously labeled intercellular F-actin and vinculin of NIH-3T3 fibroblasts cultured on either SLG or non-SLG coated substrates. It is known that F-actin and vinculin are essential components of microfilament cytoskeleton and focal adhesions, respectively, and therefore are commonly used to evaluate the cell cytoskeleton structure and adhesion [36–39]. As shown in Fig. 5, fluorescence images of F-actin (red) showed that cytoskeleton exhibited remarkable different distribution on these bare substrates. NIH-3T3 cultured on the stiffest substrates (glass and p-P10) displayed more and stronger F-actin, showing much more stress fibers and distribution along with the long axial of the cells, whereas fibroblasts cultured on stiffer substrates (silicone and P10) showed less organized actin filament. In contrast, fibroblasts adhered on softer substrate (P50) appeared dispersedly distributed actin filament in the cell cytoplasm. After SLG coating, all cultured fibroblasts exhibited clear stress fiber structures, suggesting that graphene enhanced the express and remodeling of F-actin even if the underlying substrates were P10 and P50. However, it can also be observed that stress fibers in fibroblasts grown on SLG-covered P50 were less than SLG-coated P10, let alone other stiffer substrates. These results demonstrated that SLG can promote F-actin network remodeling, which was also affected by the stiffness of underlying substrates.

As main linker between intracellular cytoskeletons and the underlying substrates [40], focal adhesions (FAs), are composed of transmembrane integrins and other integrin-associated multi-

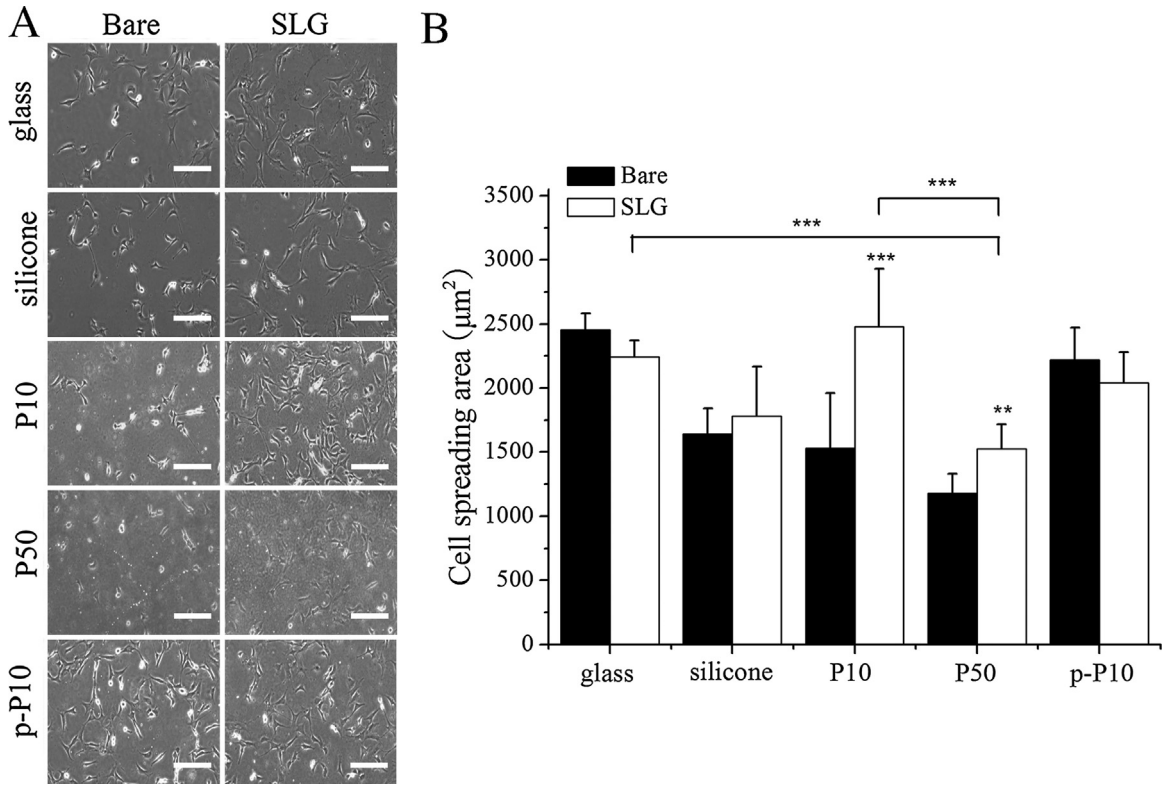

Fig. 4. Cell morphology of NIH-3T3 fibroblasts on either or not SLG coated different substrates. (A) Representative phase-contract images of NIH-3T3 fibroblasts cultured in bare and SLG-coated different substrates. (B) The quantitative cell spreading area of fibroblasts corresponding to the images shown in (A). The results showed that, compared to bare substrates, cell spreading area was increased in SLG-coated substrates. Notably, the effect of graphene on inducing cell spreading was related to the stiffness of underlying substrate, for cell spreading on SLG-coated softer substrates (P50) was still significant worse than that on SLG-coated stiffer substrate (glass and P10); scale bare = 50 μm. (**$p < 0.01$, ***$p < 0.001$, $n = 5$).

molecules including vinculin. As shown in Fig. 5, fluorescent images of vinculin (green) manifested that FA structure also exhibited remarkable different distribution on those bare substrates. Fibroblasts cultured on the stiffest substrate (bare glass and p-P10) took on typical FA structure near the periphery of cells, while those cultured on the stiffer substrate (bare silicone and P10) showed blur and immature FAs. In comparison, fibroblasts cultured on the softer substrate (bare P50) only exhibited several dot-like nascent FAs. The coverage of SLG increased the formation of FAs, as more typical matured FAs can be identified near the periphery of cells. Notably, compared to other SLG-covered substrates, especially stiffer underlying substrates (P10), FAs in cells cultured on SLG-covered softer substrate (P50) were less prominent grown.

In order to investigate the effect of the underlying substrates on SLG-induced FAs formation in a quantitative way, the area and number of FAs per cell were collected as shown in Fig. 6A and B, respectively. The outcome revealed that the area and number of FAs per cell on these bare substrates was remarkable different, which was similar to the aforementioned results. After coating with SLG, the difference was diminished, indicating that the fibroblasts have higher affinity for the graphene than for bare substrates. However, compared to other SLG-covered substrates, especially stiffer substrates (P10), the total FAs area and number per cell on SLG covered softer substrate (P50) was still significantly smaller ($p < 0.05$), meaning that the underlying substrate can still influence the SLG-induced formation of FAs.

Based on all the above experimental results, we found that SLG improved the cytocompatibility of the supported substrates. Simultaneously, the substrate stiffness effect might regulate adhesion and proliferation of fibroblast on SLG. Our findings demonstrated a coordination of biochemical and mechanical signals to regulate fibroblast adhesion and proliferation on SLG-coated substrates. The effect of graphene may come from its good adsorption ability to adsorb the proteins like fibronectin and insulin from medium to the material surface, which can enhance cell adhesion and proliferation [6,41]. On the other hand, the effect of substrate was from that substrate stiffness could alter the activation of focal adhesion proteins like integrin, vinculin, and talin to mediate the formation of focal adhesion, remodeling of cytoskeleton etc., which could further trigger a series of complex signal pathways to regulate adhesion, proliferation and differentiation of cells [42–47].

On the other hand, as the soft substrate can still exert their stiffness effect by passing through SLG, SLG-coated substrate system can be utilized to study the cell response to stiffness stimulation. The widely used method to study the cell response to stiffness stimulations are based on changing the substrate material, such as vary the curing ratio of PDMS [25,48] and polyacrylamide gels (PA) [31,49,50], which always introduce other unwanted changes, such as porosity [49] and different chemical components. However, SLG produced by CVD was the thinnest membrane that can provide homogeneous SLG for cell research, simultaneously, SLG-coated soft substrates can guarantee the homogeneous surface of composite materials and the apparent stiffness is different, which may at least provide a relative pure environment to investigate the stiffness stimulation on cell function and behaviors. Aside from changing the underlying elastic modulus to tune the apparent stiffness, it can also be modulated by transferring different layers of graphene on the identical underlying substrate. These approaches provide new possibilities to study the mechanism of cell sensing their mechanical environment.

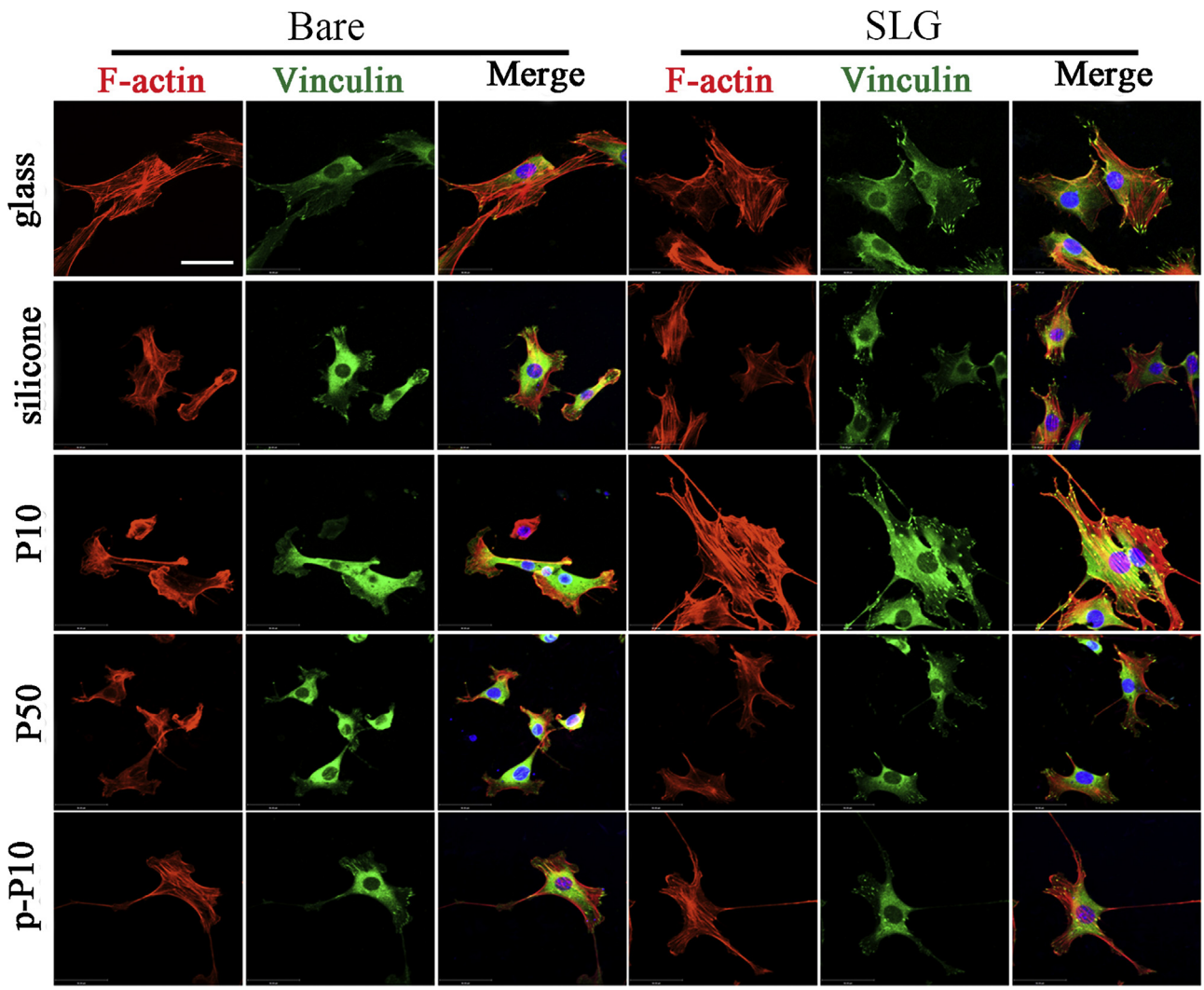

Fig. 5. Remodeling of cytoskeletal structure of NIH-3T3 fibroblasts cultured on either or not SLG coated different substrates. Fluorescent images represented the remodeled fibroblasts cytoskeleton that was characterized by fluorescently labeled F-actin (red) and vinculin (green), and visualized by confocal microscopy (×40, oil); scare bare = 50 μm. (For interpretation of the references to colour in this figure legend, the reader is referred to the web version of this article.)

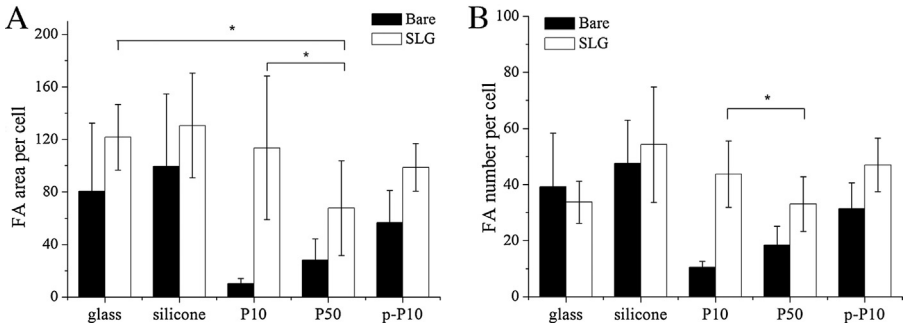

Fig. 6. Quantitative analysis of focal adhesion (FA) area per cell (A) and FA number per cell (B) of adhered NIH-3T3 fibroblasts on either or not SLG coated different substrates corresponding to the images shown in Fig. 5. The results showed that, compared to bare substrate, FA area and number were increased in SLG-coated substrates, and the enhancement was related to the stiffness of underlying substrate, for the value of FA area and number on SLG-coated softer substrate (P50) was still significant smaller and lower than that on SLG-coated stiffer substrate (glass and P10). (*$p < 0.05$, $n = 5$).

4. Conclusion

In summary, the primary finding of this study was that single-layer graphene produced by CVD had good cell compatibility and improved the substrate cytocompatibility even if the bare substrate was not originally suitable for cell growth. Notably, the adhesion and proliferation of cells such as fibroblast were not completely equivalent after single-layer graphene coating on these substrates; especially the graphene-induced cytocompatibility on softer substrate was lower than that on stiffer substrates. These results suggested that the underlying substrate effect might play an essential role in regulating adhesion and proliferation of cells like

fibroblasts on these SLG-coated soft materials. The current investigation provides a valuable guide for the design and application of graphene-based biomaterials as scaffolds for tissue engineering.

Acknowledgements

C.Y.X. acknowledges the support of the National Basic Research Program of China under Grant no. 2013CB933702 and the National Natural Science Foundation of China (NSFC) under Grant Nos. 11272015 and 11472013. H.L.D. acknowledges the support of the National Natural Science Foundation of China (NSFC) under Grants No. 11225208. C.Y.X. and Y.S.Z. acknowledge the support of Peking University 985 program.

References

[1] K.S. Novoselov, V.I. Fal'ko, L. Colombo, P.R. Gellert, M.G. Schwab, K. Kim, A roadmap for graphene, Nature 490 (2012) 192–200, http://dx.doi.org/10.1038/nature11458.
[2] A.K. Geim, Graphene: status and prospects, Science 324 (2009) 1530–1534, http://dx.doi.org/10.1126/science.1158877.
[3] H.Y. Mao, S. Laurent, W. Chen, O. Akhavan, M. Imani, A.A. Ashkarran, M. Mahmoudi, Graphene: promises, facts, opportunities, and challenges in nanomedicine, Chem. Rev. 113 (2013) 3407–3424, http://dx.doi.org/10.1021/cr300335p.
[4] X. Zhao, P. Zhang, Y. Chen, Z. Su, G. Wei, Recent advances in the fabrication and structure-specific applications of graphene-based inorganic hybrid membranes, Nanoscale 7 (2015) 5080–5093, http://dx.doi.org/10.1039/c5nr00084j.
[5] X. Yu, W. Zhang, P. Zhang, Z. Su, Fabrication technologies and sensing applications of graphene-based composite films: advances and challenges, Biosens. Bioelectron. (2016), http://dx.doi.org/10.1016/j.bios.2016.01.081.
[6] M. Gu, Y.S. Liu, T. Chen, F. Du, X.H. Zhao, C.Y. Xiong, Y.S. Zhou, Is graphene a promising nano-material for promoting surface modification of implants or scaffold materials in bone tissue engineering? Tissue Eng. Part B Rev. 20 (2014) 477–491, http://dx.doi.org/10.1089/ten.teb.2013.0638.
[7] X.L. Ding, H.F. Liu, Y.B. Fan, Adv. Healthcare Mater. 4 (2015) 1451–1468, http://dx.doi.org/10.1002/adhm.201500203.
[8] P. Zhang, H. Wang, X. Zhang, W. Xu, Y. Li, Q. Li, G. Wei, Z. Su, Graphene film doped with silver nanoparticles: self-assembly formation, structural characterizations, antibacterial ability, and biocompatibility, Biomater. Sci. 3 (2015) 852–860, http://dx.doi.org/10.1039/c5bm00058k.
[9] M. Kalbacova, A. Broz, J. Kong, M. Kalbac, Graphene substrates promote adherence of human osteoblasts and mesenchymal stromal cells, Carbon 48 (2010) 4323–4329, http://dx.doi.org/10.1016/j.carbon.2010.07.045.
[10] M. Lorenzoni, F. Brandi, S. Dante, A. Giugni, B. Torre, Simple and effective graphene laser processing for neuron patterning application, Sci. Rep. 3 (2013), http://dx.doi.org/10.1038/srep01954.
[11] T.R. Nayak, H. Andersen, V.S. Makam, C. Khaw, S. Bae, X.F. Xu, P.L.R. Ee, J.H. Ahn, B.H. Hong, G. Pastorin, B. Ozyilmaz, Graphene for controlled and accelerated osteogenic differentiation of human mesenchymal stem cells, ACS Nano 5 (2011) 4670–4678, http://dx.doi.org/10.1021/nn200500h.
[12] Y.S. Liu, T. Chen, F. Du, M. Gu, P. Zhang, X. Zhang, J.Z. Liu, L.W. Lv, C.Y. Xiong, Y.S. Zhou, Single-layer graphene enhances the osteogenic differentiation of human mesenchymal stem cells in vitro and in vivo, J. Biomed. Nanotechnol. 12 (2016) 1270–1284, http://dx.doi.org/10.1166/jbn.2016.2254.
[13] W.C. Lee, C. Lim, H. Shi, L.A.L. Tang, Y. Wang, C.T. Lim, K.P. Loh, Origin of enhanced stem cell growth and differentiation on graphene and graphene oxide, ACS Nano 5 (2011) 7334–7341, http://dx.doi.org/10.1021/nn202190c.
[14] J. Rafiee, X. Mi, H. Gullapalli, A.V. Thomas, F. Yavari, Y.F. Shi, P.M. Ajayan, N.A. Koratkar, Wetting transparency of graphene, Nat. Mater. 11 (2012) 217–222, http://dx.doi.org/10.1038/nmat3228.
[15] C.J. Shih, M.S. Strano, D. Blankschtein, Wetting translucency of graphene, Nat. Mater. 12 (2013) 866–869, http://dx.doi.org/10.1038/nmat3760.
[16] M. Garnica, D. Stradi, S. Barja, F. Calleja, C. Diaz, M. Alcami, N. Martin, A.L.V. de Parga, F. Martin, R. Miranda, Long-range magnetic order in a purely organic 2D layer adsorbed on epitaxial graphene, Nat. Phys. 9 (2013) 368–374, http://dx.doi.org/10.1038/nphys2610.
[17] S.J. Goncher, L.Y. Zhao, A.N. Pasupathy, G.W. Flynn, Substrate level control of the local doping in graphene, Nano Lett. 13 (2013) 1386–1392, http://dx.doi.org/10.1021/nl3039508.
[18] M. Lanza, Y. Wang, A. Bayerl, T. Gao, M. Porti, M. Nafria, H. Liang, G. Jing, Z. Liu, Y. Zhang, Y. Tong, H. Duan, Tuning graphene morphology by substrate towards wrinkle-free devices: experiment and simulation, J. Appl. Phys. 113 (2013), http://dx.doi.org/10.1063/1.4794521.
[19] J. Chen, X.L. Guo, Q. Tang, C.Y. Zhuang, J.S. Liu, S.Q. Wu, B.D. Beake, Nanomechanical properties of graphene on poly(ethylene terephthalate) substrate, Carbon 55 (2013) 144–150, http://dx.doi.org/10.1016/j.carbon.2012.12.020.
[20] J. Song, F.Y. Kam, R.Q. Png, W.L. Seah, J.M. Zhuo, G.K. Lim, P.K.H. Ho, L.L. Chua, A general method for transferring graphene onto soft surfaces, Nat. Nanotechnol. 8 (2013) 356–362, http://dx.doi.org/10.1038/nnano.2013.63.
[21] X.D. Chen, Z.B. Liu, C.Y. Zheng, F. Xing, X.Q. Yan, Y.S. Chen, J.G. Tian, High-quality and efficient transfer of large-area graphene films onto different substrates, Carbon 56 (2013) 271–278, http://dx.doi.org/10.1016/j.carbon.2013.01.011.
[22] Y. Wang, S.W. Tong, X.F. Xu, B. Ozyilmaz, K.P. Loh, Interface engineering of layer-by-layer stacked graphene anodes for high-performance organic solar cells, Adv. Mater. 23 (2011) 1514–1518, http://dx.doi.org/10.1002/adma.201003673.
[23] J. Kang, D. Shin, S. Bae, B.H. Hong, Graphene transfer: key for applications, Nanoscale 4 (2012) 5527–5537, http://dx.doi.org/10.1039/c2nr31317k.
[24] X.L. Shi, L. Qin, X.J. Zhang, K.M. He, C.Y. Xiong, J. Fang, X.H. Fang, Y.Y. Zhang, Elasticity of cardiac cells on the polymer substrates with different stiffness: an atomic force microscopy study, Phys. Chem. Chem. Phys. 13 (2011) 7540–7545, http://dx.doi.org/10.1039/c1cp20154a.
[25] A.I. Teixeira, S. Ilkhanizadeh, J.A. Wigenius, J.K. Duckworth, O. Inganas, O. Hermanson, The promotion of neuronal maturation on soft substrates, Biomaterials 30 (2009) 4567–4572, http://dx.doi.org/10.1016/j.biomaterials.2009.05.013.
[26] M. Versaevel, T. Grevesse, S. Gabriele, Spatial coordination between cell and nuclear shape within micropatterned endothelial cells, Nat. Commun. 3 (2012), http://dx.doi.org/10.1038/ncomms1668.
[27] A.C. Ferrari, J.C. Meyer, V. Scardaci, C. Casiraghi, M. Lazzeri, F. Mauri, S. Piscanec, D. Jiang, K.S. Novoselov, S. Roth, A.K. Geim, Raman spectrum of graphene and graphene layers, Phys. Rev. Lett. 97 (2006), http://dx.doi.org/10.1103/physrevlett.97.187401.
[28] T. Osathanon, C. Sawangmake, N. Ruangchainicom, P. Wutikornwipak, P. Kantukiti, N. Nowwarote, P. Pavasant, Surface properties and early murine pre-osteoblastic cell responses of phosphoric acid modified titanium surface, J. Oral Biol. Craniofacial Res. 6 (2016) 2–9, http://dx.doi.org/10.1016/j.jobcr.2015.12.005.
[29] M. Raab, J. Swift, P.C.D.P. Dingal, P. Shah, J.W. Shin, D.E. Discher, Crawling from soft to stiff matrix polarizes the cytoskeleton and phosphoregulates myosin-II heavy chain, J. Cell Biol. 199 (2012) 669–683, http://dx.doi.org/10.3410/f.717968593.793468382.
[30] M. Prager-Khoutorsky, A. Lichtenstein, R. Krishnan, K. Rajendran, A. Mayo, Z. Kam, B. Geiger, A.D. Bershadsky, Fibroblast polarization is a matrix-rigidity-dependent process controlled by focal adhesion mechanosensing, Nat. Cell Biol. 13 (2011) 1457–1465, http://dx.doi.org/10.1038/ncb2370.
[31] A.J. Engler, S. Sen, H.L. Sweeney, D.E. Discher, Matrix elasticity directs stem cell lineage specification, Cell 126 (2006) 677–689, http://dx.doi.org/10.1016/j.cell.2006.06.044.
[32] I. Hopp, A. Michelmore, L.E. Smith, D.E. Robinson, A. Bachhuka, A. Mierczynska, K. Vasilev, The influence of substrate stiffness gradients on primary human dermal fibroblasts, Biomaterials 34 (2013) 5070–5077, http://dx.doi.org/10.1016/j.biomaterials.2013.03.075.
[33] S. Mehrotra, S.C. Hunley, K.M. Pawelec, L.X. Zhang, I. Lee, S. Baek, C. Chan, Cell adhesive behavior on thin polyelectrolyte multilayers: cells attempt to achieve homeostasis of its adhesion energy, Langmuir 26 (2010) 12794–12802, http://dx.doi.org/10.1021/la101689z.
[34] W.S. Leong, C.Y. Tay, H.Y. Yu, A. Li, S.C. Wu, D.H. Duc, C.T. Lim, L.P. Tan, Thickness sensing of hMSCs on collagen gel directs stem cell fate, Biochem. Biophys. Res. Commun. 401 (2010) 287–292, http://dx.doi.org/10.1016/j.bbrc.2010.09.052.
[35] V. Singh, D. Joung, L. Zhai, S. Das, S.I. Khondaker, S. Seal, Graphene based materials: past, present and future, Prog. Mater. Sci. 56 (2011) 1178–1271, http://dx.doi.org/10.1016/j.pmatsci.2011.03.003.
[36] S.R. Ryoo, Y.K. Kim, M.H. Kim, D.H. Min, Behaviors of NIH-3T3 fibroblasts on graphene/carbon nanotubes: proliferation, focal adhesion, and gene transfection studies, ACS Nano 4 (2010) 6587–6598, http://dx.doi.org/10.1021/nn1018279.
[37] A. Carisey, C. Ballestrem, Vinculin, an adapter protein in control of cell adhesion signalling, Eur. J. Cell Biol. 90 (2011) 157–163, http://dx.doi.org/10.1016/j.ejcb.2010.06.007.
[38] K.A. DeMali, Vinculin – a dynamic regulator of cell adhesion, Trends Biochem. Sci. 29 (2004) 565–567, http://dx.doi.org/10.1016/j.tibs.2004.09.001.
[39] J.H.C. Wang, J.S. Lin, Cell traction force and measurement methods, Biomech. Model. Mechanobiol. 6 (2007) 361–371, http://dx.doi.org/10.1007/s10237-006-0068-4.
[40] B. Geiger, J.P. Spatz, A.D. Bershadsky, Environmental sensing through focal adhesions, Nat. Rev. Mol. Cell Biol. 10 (2009) 21–33, http://dx.doi.org/10.1038/nrm2593.
[41] Kenry, P.K. Chaudhuri, K.P. Loh, C.T. Lim, Selective accelerated proliferation of malignant breast cancer cells on planar graphene oxide films, ACS Nano 10 (2016) 3424–3434, http://dx.doi.org/10.1021/acsnano.5b07409.
[42] J. Du, X.F. Chen, X.D. Liang, G.Y. Zhang, J. Xu, L.R. He, Q.Y. Zhan, X.Q. Feng, S. Chien, C. Yang, Integrin activation and internalization on soft ECM as a mechanism of induction of stem cell differentiation by ECM elasticity, Proc. Natl. Acad. Sci. U. S. A 108 (2011) 9466–9471, http://dx.doi.org/10.1073/pnas.1106467108.
[43] L. Jiang, Z.L. Sun, X.F. Chen, J. Li, Y. Xu, Y. Zu, J.L. Hu, D. Han, C. Yang, Cells sensing mechanical cues: stiffness influences the lifetime of cell-extracellular

matrix interactions by affecting the loading rate, ACS Nano 10 (2016) 207–217, http://dx.doi.org/10.1021/acsnano.5b03157.
[44] A. Elosegui-Artola, R. Oria, Y.F. Chen, A. Kosmalska, C. Perez-Gonzalez, N. Castro, C. Zhu, X. Trepat, P. Roca-Cusachs, Mechanical regulation of a molecular clutch defines force transmission and transduction in response to matrix rigidity, Nat. Cell Biol. 18 (2016) 540–548, http://dx.doi.org/10.1038/ncb3336.
[45] J.Y. Huang, X.L. Peng, C.Y. Xiong, J. Fang, Influence of substrate rigidity on primary nucleation of cell adhesion: a thermal fluctuation model, J. Colloid Interface Sci. 366 (2012) 200–208, http://dx.doi.org/10.1016/j.jcis.2011.09.046.
[46] X.L. Peng, J.Y. Huang, C.Y. Xiong, J. Fang, Cell adhesion nucleation regulated by substrate stiffness: a Monte Carlo study, J. Biomech. 45 (2012) 116–122, http://dx.doi.org/10.1016/j.jbiomech.2011.09.013.
[47] J.Y. Huang, X.L. Peng, C.Y. Xiong, J. Fang, Influence of substrate stiffness on cell-substrate interfacial adhesion and spreading: a mechano-chemical coupling model, J. Colloid Interface Sci. 355 (2011) 503–508, http://dx.doi.org/10.1016/j.jcis.2010.12.055.
[48] P.Y. Wang, W.B. Tsai, N.H. Voelcker, Screening of rat mesenchymal stem cell behaviour on polydimethylsiloxane stiffness gradients, Acta Biomater. 8 (2012) 519–530, http://dx.doi.org/10.1016/j.actbio.2011.09.030.
[49] B. Trappmann, J.E. Gautrot, J.T. Connelly, D.G.T. Strange, Y. Li, M.L. Oyen, M.A.C. Stuart, H. Boehm, B.J. Li, V. Vogel, J.P. Spatz, F.M. Watt, W.T.S. Huck, Extracellular-matrix tethering regulates stem-cell fate, Nat. Mater. 11 (2012) 642–649, http://dx.doi.org/10.1038/nmat3339.
[50] B.C. Isenberg, P.A. DiMilla, M. Walker, S. Kim, J.Y. Wong, Vascular smooth muscle cell durotaxis depends on substrate stiffness gradient strength, Biophys. J. 97 (2009) 1313–1322, http://dx.doi.org/10.1016/j.bpj.2009.06.021.